Research paper

A microneedle roller for transdermal drug delivery

Jung-Hwan Park [a,*], Seong-O Choi [b], Soonmin Seo [a], Young Bin Choy [c], Mark R. Prausnitz [b,**]

[a] Department of BioNano Technology and Gachon BioNano Research Institute, Kyungwon University, Seongnam, Republic of Korea
[b] School of Chemical and Biomolecular Engineering, Georgia Institute of Technology, Atlanta, USA
[c] Department of Biomedical Engineering, College of Medicine and Institute of Medical & Biological Engineering, Medical Research Center,
Seoul National University, Seoul, Republic of Korea

ARTICLE INFO

ABSTRACT

Microneedle rollers have been used to treat large areas of skin for cosmetic purposes and to increase skin permeability for drug delivery. In this study, we introduce a polymer microneedle roller fabricated by inclined rotational UV lithography, replicated by micromolding hydrophobic polylactic acid and hydrophilic carboxy-methyl-cellulose. These microneedles created micron-scale holes in human and porcine cadaver skin that permitted entry of acetylsalicylic acid, Trypan blue and nanoparticles measuring 50 nm and 200 nm in diameter. The amount of acetylsalicylic acid delivered increased with the number of holes made in the skin and was 1–2 orders of magnitude greater than in untreated skin. Lateral diffusion in the skin between holes made by microneedles followed expected diffusional kinetics, with effective diffusivity values that were 23–160 times smaller than in water. Compared to inserting microneedles on a flat patch, the sequential insertion of microneedles row by row on a roller required less insertion force in full-thickness porcine skin. Overall, polymer microneedle rollers, prepared from replicated polymer films, offer a simple way to increase skin permeability for drug delivery.

© 2010 Elsevier B.V. All rights reserved.

1. Introduction

Microneedles have been introduced to increase skin permeability by creating micron-scale pathways across the skin's *stratum corneum* barrier layer, thereby permitting entry of small-molecule drugs, proteins and vaccines [1–4]. Microneedles typically measuring hundreds of microns in length can be made by leveraging microfabrication tools of the microelectronics industry for low-cost mass production. Solid microneedles have been used to pierce the skin to increase drug absorption from a patch or other topical formulations [5–8]. Solid microneedles have also been designed to be coated with a drug or to encapsulate the drug for release into the skin by dissolution [9–12]. Finally, hollow microneedles have been coupled with a syringe for active drug infusion [13–15].

This study addresses the use of solid microneedles to increase skin permeability. Previous studies have shown that skin permeability can be increased by orders of magnitude for delivery of, for example, naltrexone, insulin, antibodies, vaccines and nanoparticles [6,8,16,17]. However, most studies have used microneedle patches arranged on flat surfaces that are difficult to apply to large areas of skin due to skin deformation under the patch. Treatment of dermatological conditions, such as psoriasis, as well as various cosmetic applications, require drug delivery into large areas of skin.

To address this concern, microneedle rollers were introduced to treat large skin areas. In this scenario, microneedles are mounted on a cylindrical surface and can be rolled across the skin, such that each microneedle may pierce the skin multiple times as the roller rotates across the skin. Most uses of microneedle rollers have not involved drug delivery, but are designed to cause microdamage to the skin, which induces collagen production during the skin repair process for cosmetic purposes [18]. More recently, microneedle rollers have been proposed and studied to increase skin permeability for pharmaceutical applications [19–22].

Microneedle rollers made of stainless steel have received the most attention, but they are costly to make and are sold commercially as multiple-use devices that require cleaning. In conventional metal microneedle rollers, microneedles were made of stainless steel. In some cases, the microneedles were attached to a circular disk or formed as one unit with the circular disk, and the microneedle roller was fabricated by alternately stacking needle disks, which were prepared by etching, press work, or other suitable techniques [33,34]. Polymer microneedles produced by a micro-embossing process have also recently been introduced, but current designs are based on fabrication of individual rows of microneedles that are assembled into two-dimensional arrays

* Corresponding author. Address: Department of BioNano Technology and Gachon BioNano Research Institute, Kyungwon University, Seongnam, Geonggi-do 461-701, Republic of Korea. Tel./fax: +82 31 750 8551.
** Corresponding author. Address: School of Chemical and Biomolecular Engineering, Georgia Institute of Technology, 311 Ferst Drive, Atlanta, GA 30332, USA. Tel.: +1 404 894 5135; fax: +1 404 894 2866.
E-mail addresses: pa90201@kyungwon.ac.kr (J.-H. Park), prausnitz@gatech.edu (M.R. Prausnitz).

[23]. Previously produced microneedle rollers have had only limited function because the fabrication process was based on the UV crosslinking of needle material, hot embossing of general purpose polymer and hand assembly of microneedle arrays on a roller. We were motivated to fabricate a polymer microneedle roller out of replicated polymer film by a one-step process to provide a simple way to increase skin permeability.

The microneedle roller is easily accessible to personal users in addition to medical professionals because it is widely available. However, the misuse of microneedle rollers can cause the delivery of an overdose of drug, injury and contamination of infected skin. In spite of various demonstrations that microneedle roller treatment can increase skin permeability, there has been no systematic study of the fabrication, mechanics and drug delivery properties of the microneedle roller system.

In this study, we introduce a novel fabrication method to produce two-dimensional arrays of microneedles on a malleable substrate that can be mounted on a cylindrical roller. The advantages of this method are easy fabrication, enhanced safety, simple integration with a roller, mass production and wide choice of needle material. Unlike previous polymer microneedle roller designs, these microneedles are made out of biodegradable polylactic acid (PLA) and water-soluble carboxy-methyl-cellulose (CMC). PLA provides additional safety in case microneedles accidentally break in the skin. CMC dissolves within the skin for sustained release and leaves encapsulating material behind in the skin. This method allows the fabrication of microneedles out of various materials, including hydrophobic thermoplastics, hydrophilic thermoplastics and hydrophilic hydrogels. Although the integration of microneedle structures on a roller is not easy because of the micron-scale size and mechanical weakness of the microneedles. The new fabrication process is simple and efficient. Two-dimensional arrays of microneedles are prepared using a simple and economic micromolding process on a flat surface of film. A layer of microneedles is wrapped around a roller, and the microneedles are fixed at the specific position.

Our study further examines the mechanical and drug delivery properties of the microneedle roller to assess its optimal use in applications.

2. Materials and methods

2.1. Fabrication of the microneedle roller

The fabrication process consisted of the preparation of a mold of a microneedle roller (process I) and the replication of polymer by micromolding (process II), as shown in Fig. 1. Process I involved steps for preparation of a PDMS female mold with microneedle cavities and a base structure by inclined rotational UV lithography and micromolding of PDMS. Process II produced a replica of microneedles by micromolding PLA (II-h process) and solvent casting CMC (II-i process) from the mold prepared by process I.

A female master mold was prepared using a photolithographic process with an SU-8 epoxy photoresist (MicroChem, Newton, MA). To make the female master mold, an SU-8 layer was spin coated (1 mm thick) onto a clean silicon wafer, baked at 95 °C for 18 h and then exposed to UV light (365 nm wavelength, 9 W/cm^2) through a mask patterned with 250 μm diameter holes. The UV exposure was carried out at an angle of 20° while the sample was rotated at 20 rpm for 900 sec, which produced a cone of non-crosslinked SU-8 [24]. The SU-8 mold was finally formed by developing the non-crosslinked SU-8 in propylene glycol methyl ether acetate (PGMEA) for 3 h. A male master structure was made out of poly-di-methyl-siloxane (PDMS, Sylgard 184, Dow Corning, Midland, MI) from the female master mold. Finally, a PDMS female mold was molded from the male master structure.

To make the final microneedle devices, the female molds were covered with pellets of polylactic acid (L-PLA, 1.1 dL/g; Lakeshore Biomaterials, Birmingham, AL) and placed in a vacuum oven (Eyeler, Tokyo Rikakikai, Japan) under −70 kPa vacuum for 5 min at 190 °C. The vacuum was applied to remove bubbles trapped in the melted polymer and to push the polymer into the cavities of the mold. PLA microneedles mounted on an 800 μm thick PLA film were removed from the PDMS mold after the sample was cooled.

Cylindrical aluminum tubes (Metals Depot, Winchester, KY) with 1 cm diameter were heated to 150 °C in an oven (Eyeler). PLA microneedle arrays were then applied to the hot tubes and, upon softening from the heat, were wrapped around them. After cooling to room temperature, the microneedle arrays were glued to 1 cm diameter aluminum cylinders to form PLA microneedle rollers.

Low viscosity CMC Sigma–Aldrich, Milwaukee, WI) was dissolved in distilled water up to 20% (w/w) at 80 °C for 6 h and then cooled to obtain CMC gel. To mold microneedles from the gel, 2 g of gel with Trypan blue (0.01% w/w) was put on the PDMS roller mold with 1200 microneedle cavities and a layer 20 mm wide, 50 mm long and 0.8 mm thick; masking tape with a few hundred micro-size holes (3 M) covered the mold to achieve uniform thickness of CMC film by preventing the overflow out of the mold while the gel was being centrifuged. The mold was placed in a centrifuge basket (Hanil Science Industry, Combi, Korea) and centrifuged at a 90° angle with 4500 g of centrifugal relative force at 25 °C for 8 h to fill the microneedle cavities in the mold and obtain dried CMC needles. The CMC layer with microneedle arrays was then applied to the wet tube and was wrapped around the roller after the layer was softened with absorbed water. After drying, the microneedle arrays were fixed on the roller using glue.

2.2. Mechanics of the microneedle roller

To assess the force required for insertion into skin, 100 microneedles arranged in a flat, 10 by 10 array, were pressed against full-thickness porcine skin at a rate of 200 μm/s with a predetermined maximum load of 5 N using a displacement-force station (Model 921A, Tricor Systems, Elgin, IL). In an alternate scenario, the microneedle roller was pressed against the skin without rolling, such that only a few rows of needles could contact the skin, under the same conditions.

To assess microneedle penetration into the skin, Trypan blue solution (0.4%, Sigma Chemical, St. Louis, MO) was applied to the skin surface before and during microneedle insertion. Treated skin samples were immersed in a freezing block filled with Tissue-Tek Optimal Cutting Temperature solution (Sakura Finetechnical, Tokyo, Japan), which was repeatedly placed in contact with a liquid nitrogen bath in 5-s increments until the skin was frozen. After storage in a −70 °C freezer, the frozen blocks were sectioned using a cryostat microtome (HM 560, Microm, Walldorf, Germany) and examined by brightfield microscopy (IX-70, Olympus, Tokyo, Japan) to image the distribution of Trypan blue in the skin.

To visualize holes made by microneedles in living human skin, microneedles were pressed into the skin of a human subject, and a liquid bandage (Skin-Shield, Del Pharmaceuticals, Farmingdale, NY) was applied 0 min, 15 min and 30 min afterwards to make an inverse replica of the holes by *in situ* molding of the skin. The resulting films were gold coated for imaging by scanning electron microscopy (3500H, Hitachi, Tokyo, Japan). This human study was approved by the Georgia Tech Institutional Review Board.

2.3. Increased skin permeability using the microneedle roller

2.3.1. Drug transport across human epidermis
To measure changes in skin permeability after treatment with a microneedle roller, we first isolated heat-stripped epidermis from
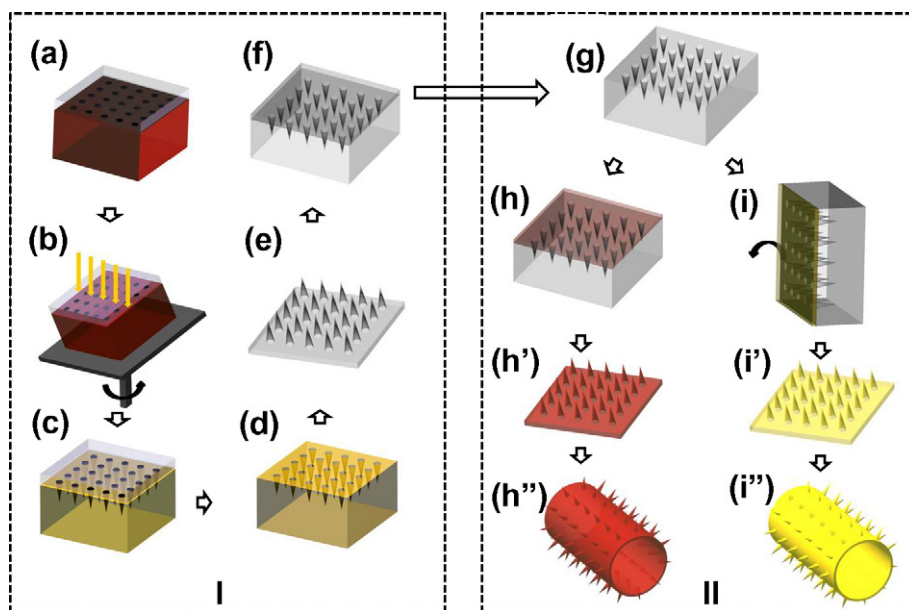
Fig. 1. Diagram of fabrication process of polymer microneedle roller from film. (a) Application of SU-8 onto an Si wafer and aligning sample with a photomask, (b) inclined rotational UV exposure, (c) cones of non-crosslinked SU-8 under photomask, (d) removal of non-crosslinked conical region, (e) male master structure made out of PDMS, (f) preparation of PDMS female mold from PDMS male master, (g) PDMS female mold, (h) cover with PLA on the PDMS mold and molding PLA in vacuum oven, (h′) thermally molded PLA microneedles, (h″) microneedle roller prepared by thermal softening of PLA film, (i) centrifugation of PDMS mold covered with CMC gel, (i′) solvent-casted CMC microneedles, and (i″) microneedle roller prepared by moisture softening CMC film.

human cadaver skin (Hans Biomed, Taejon, Korea). Epidermis was used because the *stratum corneum* (i.e., the upper layer of epidermis) is the primary barrier to transdermal transport [25], as well as the main mechanical barrier to needle insertion [26].

Epidermis was placed on ten layers of tissue paper (Kimwipes, Kimberly-Clark, Neenah, WI) to provide a tissue-like mechanical support, and a microneedle roller was rolled once across the epidermis using a force of 10 N and removed. The force was determined by placing the epidermis on a balance, which applied the microneedle roller. The epidermis was then loaded into a Franz diffusion chamber (Permegear, Hellertown, PA), which was immersed in a 32 °C water bath (Cole Parmer, Vernon Hills, IL) with magnetic stirring (Immersible multi-stirrer, Cole Parmer). The lower receptor compartment was filled with 5 ml of well-stirred, phosphate-buffered saline (PBS) in contact with the underside of the viable epidermis. The upper donor compartment in contact with the *stratum corneum* was initially filled with PBS for 2 h to permit skin hydration, after which it was filled with 0.5 ml of 0.2% w/v acetylsalicylic acid (SA; Sigma Chemical) in PBS. Two hours later, 1 ml of receptor solution was sampled. The concentration of SA in the receptor solution was quantified by absorbance at 290 nm by calibrated UV spectrophotometry (Multilabel Readers Victor[3], Perkin Elmer, Eden Prairie, MN), and the amount of SA transferred into the receptor solution was calculated.

2.3.2. Drug transport into porcine skin

In additional experiments, microneedle rollers were applied to full-thickness porcine skin with 10 N force. Then, a donor chamber (Permegear) was adhered to the *stratum corneum* side of the skin using epoxy adhesive (Araldite, Huntsman, Salt Lake City, UT). A total of 0.5 ml of 0.2% w/v SA in PBS were placed in the donor chamber and maintained at 32 °C in an incubator for 2 h. Then, the skin was cut into pieces approximately 1.5 cm in size and frozen in liquid nitrogen. A frozen skin sample was pulverized into particles measuring a few hundred microns in size (Shinko Seiki, Fukuoka, Japan) and incubated in a solution of 94% distilled water, 5.6% acetonitrile, 0.2% triethylamine and 0.2% acetic acid (Sigma–Aldrich) for 12 h at room temperature to extract SA from the skin. The con-

centration of extracted SA was quantified by injecting 20 μl of the extracted solution supernatant into a 3.9 mm × 30 cm C18 column of an HPLC (Agilent 1200, Santa Clara, CA) using a mobile phase of 94% distilled water, 5.6% acetonitrile, 0.2% triethylamine and 0.2% acetic acid at a flow rate of 1.0 ml/min. Detection was carried out at 290 nm. The retention time for SA was approximately 13 min. The amount of SA was determined by measuring its peak height and comparing this with a calibration curve.

2.3.3. Drug diffusion within human skin

Diffusion lateral to the skin surface in microneedle-treated skin was investigated as a function of molecule/particle size and time at 32 °C. The microneedle roller was applied to human cadaver skin with a force of 10 N. Then, 100 μl of 0.4% w/v Trypan blue (961 Da, Sigma Chemical) or 2.5% w/v fluorescent nanospheres with 50 nm or 200 nm diameter (Fluorosbrite, Polysciences, Warrington, PA) was placed on the skin for 5–50 min in an incubator at 32 °C. The diffusional spread area of these compounds was measured by optical microscopy for Trypan blue (Nikon Eclipse 80i, Nikon Instruments, Melville, NY) and fluorescence microscopy for fluorescent nanoparticles (TE-2000, Nikon Instruments).

3. Results

3.1. Fabrication of the microneedle roller

Microneedle rollers were fabricated by first making a master structure by rotational UV lithography, replicating the master structure in PLA using micromolding and finally mounting the PLA microneedles onto a cylindrical roller for application to the skin. The master structure of the microneedle shape was determined by controlling the angle of UV exposure, taking into account the refractive index of the lithographic material. Specifically, Snell's law determines that light shined at a 20° angle through air with a refractive index of 1.00 passes through a film of SU-8 photolithographic polymer with a refractive index of 1.67 at an angle of 78.3° relative to the film surface. Using masks with an array

of 250 μm circular dots or 250 μm square dots, and rotating the polymer film during exposure traces out an array of cones of light in the polymer film measuring 600 μm in height and 250 μm in base diameter, which form the microneedle mold after development. This UV inclined rotation method provides a uniform geometry of the master structure of the microneedles over a large area of a few square centimeters, and the various shapes of the master structure of the microneedles can be prepared by changing masks, as shown in Fig. 2b and c.

Using this approach, master structures were fabricated and copied using micromolding to produce replica microneedle arrays as shown in Fig. 2a and b for PLA needles and Fig. 2c and d for CMC needles. These replica microneedles were fabricated out of PLA and CMC because they are biologically safe, have sufficient mechanical strength and are straightforward to process [27,28]. The resulting 20 × 60 array contained 1200 microneedles with a center-to-center spacing of 850 μm on a base substrate also made of PLA measuring 2 cm × 5 cm × 0.05 cm, as shown in Fig. 2a. Facilitated by temporary softening at elevated temperature, the microneedle array was adhered conformally onto a 1 cm diameter cylinder to make the microneedle roller, as shown in Fig. 2e and f.

The microneedle roller was fabricated with CMC gel using micromolding to deliver the active ingredient into the skin by the single step of rolling without additional application of a topical formulation. The CMC-based dissolving microneedle array was prepared by solvent casting with aqueous CMC gel, as shown in Fig. 2c. The CMC microneedle encapsulated Trypan blue in the dissolving needle structures, as shown in Fig. 2d. The fabrication of the roller structure requires a relatively large molding area of a few square centimeters and uniform casting over the surface of the mold. Thus, a 90° angled rotation, a thin wall 0.5 mm high around the mold and masking tape containing tiny pores were used to make the layer with a uniform thickness. A polymer melt of thermoplastics and polymer gel of hydrophilic polymer filled the cavities and formed a thin layer over a large area, enabling the polymer microneedle roller to be prepared by a two-step process: (1) micromolding a film with microneedles and (2) wrapping the film around the roller. This microneedle roller can be used to pierce holes into the skin to deliver the drug over a large skin area. Compared to the PDMS male master structure, the final structure of PLA on the flat film had the same geometries as the master structure. However, the solvent casting of CMC reduced the base diameter by volumetric shrinkage induced by water evaporation, and the extent of shrinkage depended on the dehydration rate of water. Also, no significant change in sharpness was found in either fabrication process, and neither was any change found in the geometry of the microneedles after conversion from film to roller.

3.2. Mechanics of the microneedle roller

Previous studies have shown that the force required to insert a microneedle array into the skin scales linearly with the surface
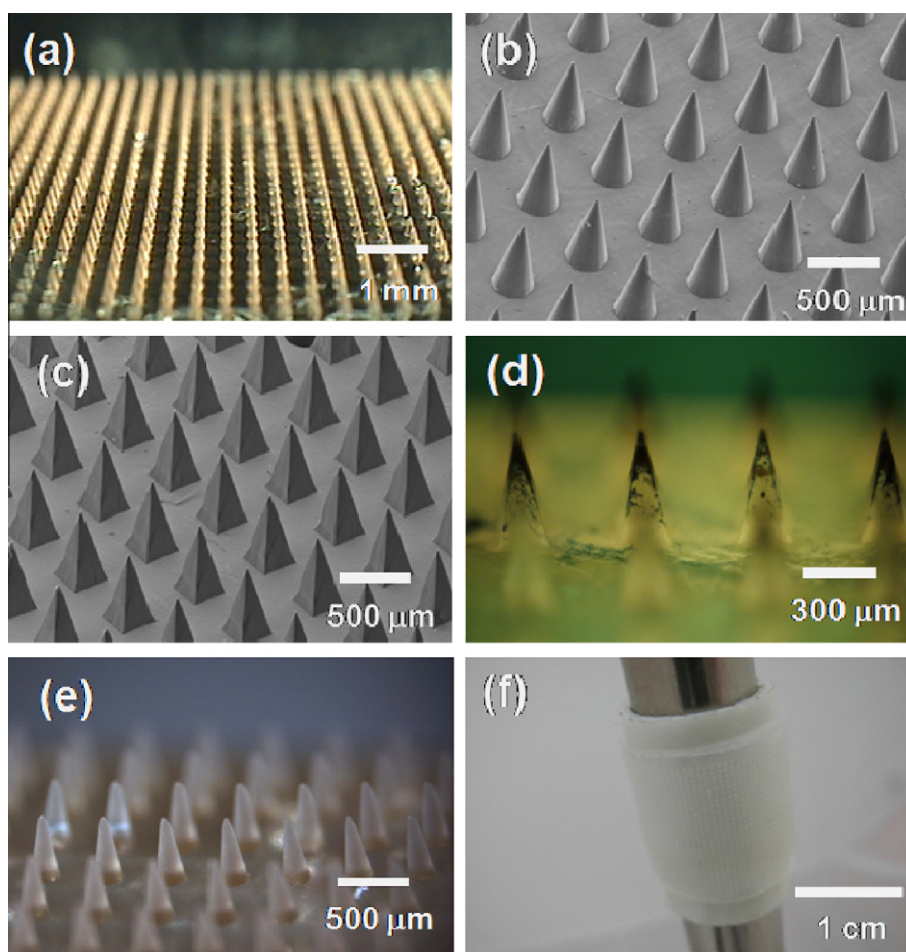

Fig. 2. Polymer microneedles and microneedle roller. Array of PLA microneedles measuring 600 μm in height and 250 μm in base diameter shown by (a) light microscopy and (b) scanning electron microscopy. Array of CMC microneedles measuring 600 μm in height and 250 μm in base width shown by (c) scanning electron microscopy and (d) light microscopy. Array of polymer microneedles mounted on a cylindrical roller with a 1 cm diameter shown by light microscopy at (e) higher and (f) lower magnification.

area of contact between the skin and the microneedle tip and with the number of microneedles [26,29]. Thus, the skin area that can be treated using a conventional planar microneedle patch is limited by the number of microneedles of a given tip sharpness that can be pressed into the skin by the force of hand insertion, or possibly through the use of an insertion device. In contrast, the microneedle roller should be able to treat much larger skin areas because only a fraction of the microneedles on the device are inserted at any given time as the microneedles roll across the skin. Based on previous analysis [26,29], a planar array of 100 microneedles with 30 μm diameter tip, 250 μm diameter base and 600 μm height is expected to require a force of approximately 8.5 N, corresponding to 0.085 N per needle, to pierce the skin. In the case of the microneedle roller, only two or three rows of microneedles at a time contact the skin and therefore a much lower force is needed, although that force must be applied for a longer time as the roller moves across the skin.

To validate these expectations, we pressed a 100-microneedle array against full-thickness porcine skin with a 5 N force, corresponding to 0.05 N per needle, and found that they did not pierce the skin, as shown in Fig. 3a. In contrast, when a roller covered with microneedles of the same geometry was applied to the skin with a force of 5 N, or 0.17 N per needle, the row of microneedles in direct contact with the skin penetrated fully, and the two adjacent rows of microneedles also penetrated (Fig. 3b). Although the controlled force apparatus used in this experiment precluded rolling, applying a force of 5 N continuously while rolling the microneedles across the skin can cover a large skin area with a force easily applied by hand. Fig. 4 illustrates this idea by showing a histological section of skin after treatment with a microneedle roller and subsequent staining to identify the sites of microneedle penetration generated by manual operation of the roller.

We were also interested in the lifetime of holes made in the skin using microneedles. After microneedles were applied across the forearm of a human subject, skin puncture holes were non-invasively imaged by applying a liquid bandage at 0 min, 15 min and 30 min after microneedle treatment to create an inverse replica of the skin surface, thereby showing the holes in the skin (Fig. 5). The initial holes had a diameter of approximately 100 μm and appeared to be relatively deep, although the tip was poorly copied, suggesting that the bottom of hole was wet due to the interstitial fluid in the skin. After 15 min, the hole opening was almost the same diameter, but its apparent depth had decreased, presumably due to elastic recoil of the tissue and possible active repair processes. After 30 min, the hole was still smaller. These kinetics of recovery are similar to those reported previously [7], although we believe these are the first images showing the skin resealing process in a human subject.
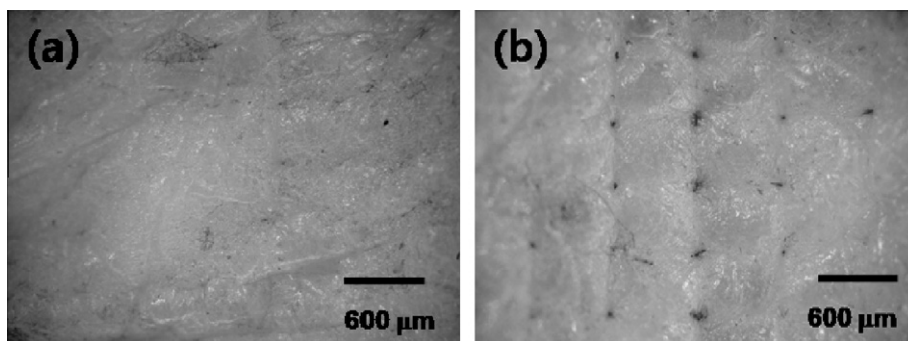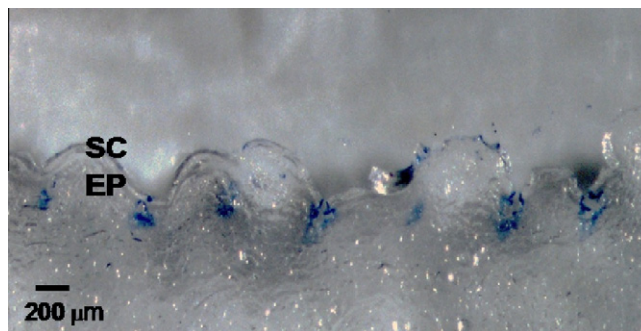

Fig. 4. Optical micrograph showing a histological section of porcine skin after insertion (with 10 N force) and removal of a row of microneedles on a roller and subsequent application of Trypan blue to the skin surface for 10 min. The blue staining shows sites of microneedle penetration into skin. SC: *stratum corneum*, EP: viable epidermis. (For interpretation of the references to colour in this figure legend, the reader is referred to the web version of this article.)

3.3. Increased skin permeability using the microneedle roller

Our goal for the microneedle roller is to increase skin permeability for transdermal drug delivery. We therefore measured skin permeability to a model drug, acetylsalicylic acid (SA), which has been used to treat hypertension, blood coagulation and restenosis, and has been proposed for transdermal delivery to reduce the side effects of oral delivery [30]. While there is a measurable flux of SA across intact human epidermis, treatment with a microneedle roller to create 100 holes in the skin increased transdermal delivery of SA by 21-fold, and creation of 200 holes increased delivery by 47-fold during the 2-h experiment, as shown in Fig. 6a.

We carried out a parallel experiment measuring delivery of SA to full-thickness pig skin by measuring the amount of SA delivered into the skin after 2 h. Similar to the experiment with human epidermis, treatment with microneedles to make 100 holes increased SA delivery by 14-fold as shown in Fig. 6b, although the absolute amount delivered into the full-thickness pig skin was almost one fourth smaller than for human epidermis. This difference may be explained by the presence of dermis in the full-thickness pig skin, which could provide elastic recoil forces that help reseal holes made by microneedles and also provide an added diffusional barrier to SA delivery. Lower measured transdermal delivery in the full-thickness pig skin could also result from incomplete extraction of SA from the skin.

3.4. Lateral diffusion in skin after microneedle treatment

Microneedles provide an array of dispersed holes in the skin. Sometimes, especially for dermatologic indications, a uniform

Fig. 3. Human cadaver skin showing the sites of microneedle insertion. Microneedles measuring 600 μm in height and 250 μm in base diameter were pressed against the skin with a force of 5 N either (a) on a flat patch (see Fig. 1a) or (b) on a cylindrical roller (see Fig. 1f). Microneedles on the roller were able to pierce the skin, whereas microneedles on the patch were not.
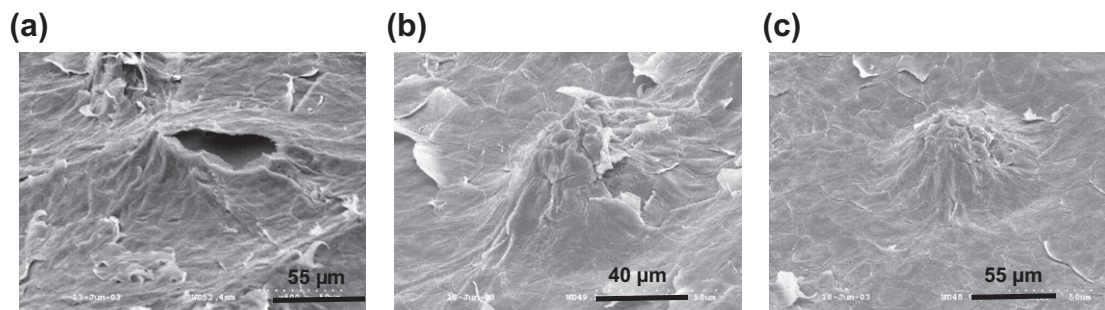
Fig. 5. Scanning electron micrographs of inverse molds showing changes in hole size after inserting and removing microneedles into the skin of a human subject at (a) 0 min, (b) 15 min and (c) 30 min after microneedle application. As an inverse mold, the height of the protrusion in the image is a measure of the depth of the hole in skin.
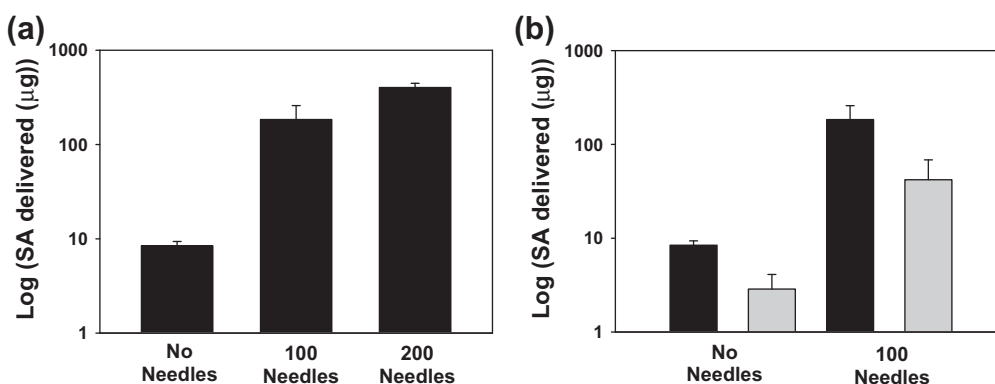

Fig. 6. Amount of SA delivered across human epidermis (a) as function of the number of microneedles (black bars) and (b) in comparison with full-thickness porcine skin (gray bars).

spread of the administered drug within the skin is desirable. We therefore investigated the lateral spread of model compounds within the skin between the holes generated by a microneedle roller. Fig. 7 shows the diffusion of a model hydrophilic molecule, Trypan blue, as a function of time after treating human cadaver skin with a microneedle roller having 600 μm center-to-center spacing. Over time, the Trypan blue diffused radially from the sites of skin puncture. The relatively slow radial diffusion shows that achieving uniform drug distribution in the skin takes time and depends on the hole-to-hole spacing. Closer spacing can be achieved by increasing microneedle density, which can make microneedle insertion more difficult, or by repeatedly rolling microneedles over the same area of skin, which can damage microneedles if they are not strong enough to withstand repeated use.

We next quantified the lateral spread as a function of time and size of the compounds administered. As shown in Fig. 8, the area of

spreading for Trypan blue and nanoparticles of 50 nm and 200 nm diameter increased approximately linearly in time, as expected for diffusion according to Fick's Law [31]. Using the formula $D = A/2\pi t$, where D is diffusivity, A is area of spreading and t is time, we calculated the effective diffusivities to be 4.1×10^{-8} cm^2/s, 3.8×10^{-9} cm^2/s and 7.6×10^{-10} cm^2/s for the Trypan blue, 50-nm particles and 200-nm particles, respectively. The Stokes–Einstein equation [32] predicts diffusivities in water at 32 °C to be 6.8×10^{-6} cm^2/s, 8.9×10^{-8} cm^2/s and 2.2×10^{-8} cm^2/s, respectively. The diffusivities in the skin are 23–160 times lower than in water, which indicates significant hindrance to diffusion in the skin.

4. Discussion of significance

Microneedles are easily accessible to patients because of their simplicity, low cost and ease of use. For this reason, microneedles
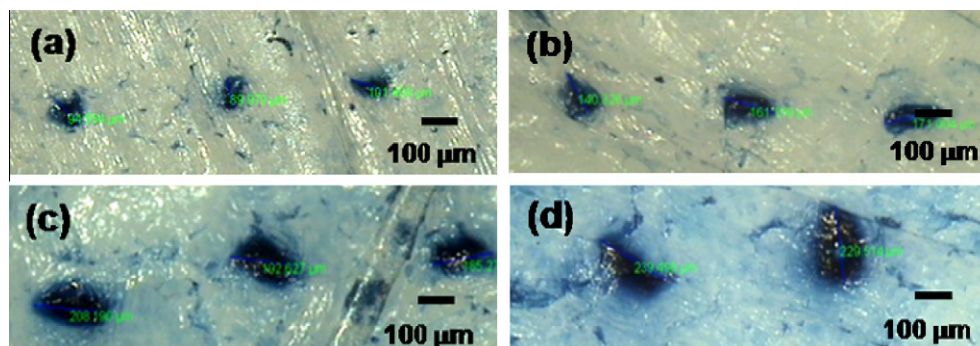

Fig. 7. *En face* images of human cadaver skin showing lateral diffusion of Trypan blue at sites of microneedle penetration as a function of time: (a) 5 min, (b) 10 min, (c) 30 min and (d) 50 min.
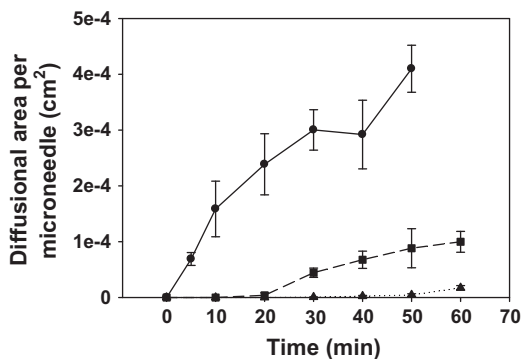
Fig. 8. Area of diffusional spread of Trypan blue (●), 50 nm diameter nanoparticles (■), and 200 nm diameter nanoparticles (▲) from sites of microneedle penetration in full-thickness porcine skin as a function of time.

have potential to be used for a variety of medical and cosmetic applications. However, a significant limitation of conventional patch-like microneedles is the difficulty in treating large areas. The microneedle roller can address this problem by rolling over large areas of skin using a simple device. While previous studies have mostly emphasized metal microneedles, which are more expensive to make, in this study we introduced a novel fabrication method to make a polymer microneedle roller that was effective to pierce skin and increase skin permeability. A CMC microneedle roller showed the possibility of delivering drugs into a large area of skin by a single roll.

Part of the reason the microneedle roller is well suited for treating large skin areas is that it minimizes the required insertion force by piercing microneedles sequentially into the skin row by row, rather than trying to force them all in at once, as is typically done with a conventional microneedle patch. However, partial mechanical failure was found at the boundary of the roller due to the angle of force applied to the microneedles by deformed skin. Thus, the needle geometry determining the mechanical stability of microneedles should be considered according to the position of the microneedles on the roller.

The microneedle rolling method consists of a two-step process of generating holes in the skin and then applying a topical formulation that delivers the drug through holes for a PLA microneedle roller and as a single-step process for a CMC microneedle roller. The amount of drug administered into the skin is determined by the number of holes, which can be controlled by the microneedle roller design and the number of times it is rolled on the skin, as well as the drug concentration, formulation and other factors. However, the dissolution of a whole CMC microneedle in the skin took a few minutes, and just few seconds of insertion of a CMC needle produced local surface erosion. Thus, accelerated erosion is necessary for the roller type of CMC microneedle to deliver the drug as designed.

If uniform distribution of the drug within the skin is needed, then the slow rate of lateral drug diffusion within the skin may require closely spaced needles or multiple passes of the roller to increase hole density.

In conclusion, this study presents a simple microneedle roller fabrication method based on micromolding a master structure generated by inclined rotational UV lithography and mounting the replicate film with PLA microneedles and CMC microneedles onto a cylindrical roller. These microneedles were found to pierce the skin with small application force, increase skin permeability to SA by 1–2 orders of magnitude and permit entry and lateral diffusion of a small molecule and polymeric nanoparticles. Altogether, these results suggest that the microneedle roller offers a useful approach to increase skin permeability for medical and other applications.

References

[1] M.R. Prausnitz, J.A. Mikszta, M. Cormier, A.K. Andrianov, Microneedle-based vaccines, Curr. Top. Microbiol. Immunol. 333 (2009) 369–393.
[2] A.K. Banga, Microporation applications for enhancing drug delivery, Expert Opin. Drug Deliv. 6 (2009) 343–354.
[3] S. Coulman, C. Allender, J. Birchall, Microneedles and other physical methods for overcoming the stratum corneum barrier for cutaneous gene therapy, Crit. Rev. Ther. Drug 23 (2006) 205–258.
[4] R.K. Sivamani, D. Liepmann, H.I. Maibach, Microneedles and transdermal applications, Expert Opin. Drug Deliv. 4 (2007) 19–25.
[5] W. Lin, M. Cormier, A. Samiee, A. Griffin, B. Johnson, C.L. Teng, G.E. Hardee, P.E. Daddona, Transdermal delivery of antisense oligonucleotides with microprojection patch (Macroflux) technology, Pharm. Res. 18 (2001) 1789–1793.
[6] D.V. McAllister, P.M. Wang, S.P. Davis, J.H. Park, P.J. Canatella, M.G. Allen, M.R. Prausnitz, Microfabricated needles for transdermal delivery of macromolecules, nanoparticles: fabrication methods and transport studies, Proc. Natl. Acad. Sci. USA 100 (2003) 13755–13760.
[7] D.P. Wermeling, S.L. Banks, D.A. Hudson, H.S. Gill, J. Gupta, M.R. Prausnitz, A.L. Stinchcomb, Microneedles permit transdermal delivery of a skin-impermeant medication to humans, Proc. Natl. Acad. Sci. USA 105 (2008) 2058.
[8] Z. Ding, F.J. Verbaan, M. Bivas-Benita, L. Bungener, A. Huckriede, D.J. van den Berg, G. Kersten, J.A. Bouwstra, Microneedle arrays for the transcutaneous immunization of diphtheria and influenza in BALB/c mice, J. Control. Release 136 (2009) 71–78.
[9] H.S. Gill, M.R. Prausnitz, Coated microneedles for transdermal delivery, J. Control. Release 117 (2007) 227–237.
[10] A.K. Andrianov, D.P. DeCollibus, H.A. Gillis, H.H. Kha, A. Marin, M.R. Prausnitz, L.A. Babiuk, H. Townsend, G. Mutwiri, Poly [di (carboxylatophenoxy) phosphazene] is a potent adjuvant for intradermal immunization, Proc. Natl. Acad. Sci. USA 106 (2009) 18936.
[11] J.W. Lee, J.-H. Park, M.R. Prausnitz, Dissolving microneedles for transdermal drug delivery, Biomaterials 29 (2008) 2113–2124.
[12] Y. Ito, E. Hagiwara, A. Saeki, N. Sugioka, K. Takada, Feasibility of microneedles for percutaneous absorption of insulin, Eur. J. Pharm. Sci. 29 (2006) 82–88.
[13] R.K. Sivamani, B. Stoeber, G.C. Wu, H. Zhai, D. Liepmann, H. Maibach, Clinical microneedle injection of methyl nicotinate: stratum corneum penetration, Skin Res. Technol. 11 (2005) 152–156.
[14] J. Gupta, E.I. Felner, M.R. Prausnitz, Minimally invasive insulin delivery in subjects with type 1 diabetes using hollow microneedles, Diabetes Technol. Ther. 11 (2009) 329–337.
[15] J.A. Mikszta, P.E. Laurent, Cutaneous delivery of prophylactic and therapeutic vaccines: historical perspective and future outlook, Expert Rev. Vaccines 7 (2008) 1329–1339.
[16] G. Li, A. Badkar, S. Nema, C.S. Kolli, A.K. Banga, In vitro transdermal delivery of therapeutic antibodies using maltose microneedles, Int. J. Pharm. 368 (2009) 109–115.
[17] W. Martanto, S.P. Davis, N. Holiday, J. Wang, H. Gill, M.R. Prausnitz, Transdermal delivery of insulin using microneedles in vivo, Pharm. Res. 21 (2004) 947–952.
[18] P. Shivanand, P. Binal, D. Viral, K. Shaliesh, G. Manish, V. Subhash, Microneedle: various techniques of fabrications and evaluations, Int. J. ChemTech Res. 1 (2009) 1058–1062.
[19] S.K. You, Y.W. Noh, H.H. Park, M. Han, S.S. Lee, S.C. Shin, C.W. Cho, Effect of applying modes of the polymer microneedle-roller on the permeation of l-ascorbic acid in rats, J. Drug Target. (2009) 1–6.
[20] G. Li, A. Badkar, H. Kalluri, A.K. Banga, Microchannels created by sugar and metal microneedles: characterization by microscopy, macromolecular flux and other techniques, J. Pharm. Sci. (2009).
[21] M.M. Badran, J. Kuntsche, A. Fahr, Skin penetration enhancement by a microneedle device (Dermaroller®) in vitro: dependency on needle size and applied formulation, Eur. J. Pharm. Sci. 36 (2009) 511–523.
[22] J. Yoon, T. Son, E. Choi, B. Choi, J.S. Nelson, B. Jung, Enhancement of optical skin clearing efficacy using a microneedle roller, J. Biomed. Opt. 13 (2008) 021103.

[23] M. Han, D.H. Hyun, H.H. Park, S.S. Lee, C.H. Kim, C.G. Kim, A novel fabrication process for out-of-plane microneedle sheets of biocompatible polymer, J. Micromech. Microeng. 17 (2007) 1184–1191.

[24] S.-O. Choi, S. Rajaraman, Y.-K. Yoon, X. Wu, M.G. Allen, 3-D Metal patterned microstructure using inclined UV exposure and metal transfer micromolding technology, in: Hilton Head 2006: A Solid State Sensors, Actuators and Microsystems Workshop, Hilton Head Island, SC, 2006.

[25] M.R. Prausnitz, R. Langer, Transdermal drug delivery, Nat. Biotechnol. 26 (2008) 1261–1268.

[26] S.P. Davis, B.J. Landis, Z.H. Adams, M.G. Allen, M.R. Prausnitz, Insertion of microneedles into skin: measurement and prediction of insertion force and needle fracture force, J. Biomech. 37 (2004) 1155–1163.

[27] J.H. Park, M.G. Allen, M.R. Prausnitz, Biodegradable polymer microneedles: fabrication, mechanics and transdermal drug delivery, J. Control. Release 104 (2005) 51–66.

[28] J.H. Park, M.G. Allen, M.R. Prausnitz, Polymer microneedles for controlled-release drug delivery, Pharm. Res. 23 (2006) 1008–1019.

[29] J.H. Park, Y.K. Yoon, S.O. Choi, M.R. Prausnitz, M.G. Allen, Tapered conical polymer microneedles fabricated using an integrated lens technique for transdermal drug delivery, IEEE Trans. Bio-Med. Eng. 54 (2007) 903–913.

[30] H.O. Ammar, M. Ghorab, S.A. El-Nahhas, R. Kamel, Design of a transdermal delivery system for aspirin as an antithrombotic drug, Int. J. Pharm. 327 (2006) 81–88.

[31] C. Washington, Drug Release from Microparticulate Systems, Marcel Dekker, New York, 1996.

[32] P. Atkins, J. dePaula, Physical Chemistry for the Life Sciences, W.H. Freeman & Company, San Francisco, 2009.

[33] K.K. Jang, Skin Perforating Device for Transdermal Medication, USA patent no., 56, 11, 806, 1997.

[34] T. James, Apparatus, System, and Method to Deliver Optimal Elements in order to Enhance the Aesthetic Appearance of the Skin, USA patent application no. 2007 0073217, 2007.